

Supporting Information

DL-Methionine-mediated radical-promoted cationic polymerization enabling the polymerization of allyl ethers

Qi Feng,^a Liyao Shi,^a Yanhua Zhang,^a Shilong Liu,^a Lumin Yang,^a Junqing Jiang,^{a,*}
and Yanwu Zhang^{a,*}

^a School of Chemical Engineering, Zhengzhou University, Zhengzhou 450001, China



Fig. S1 Schematic of the reactor setup for photoinduced polymerization.

Table S1 Additional results of the FRPCP of PEG-AME using HMPP

Entry	[M]:[Met]:[HMPP]:[DPI]	Solvent	Conv.(%)	$M_{n,th}/g \cdot mol^{-1}$	$M_{n,H\ NMR}/g \cdot mol^{-1}$	DP
1	40:1:1:1	DCM:THF=7:3	64.6	17700	14500	21.3
2	20:1:0:1	DCM:THF=7:3	0	0	0	0
3	20:1:1:1	DCM:BTF=7:3	18.55	2700	2500	3.4
4	20:1:1:1	DCM:DCE=7:3	17.93	2600	2200	3.0

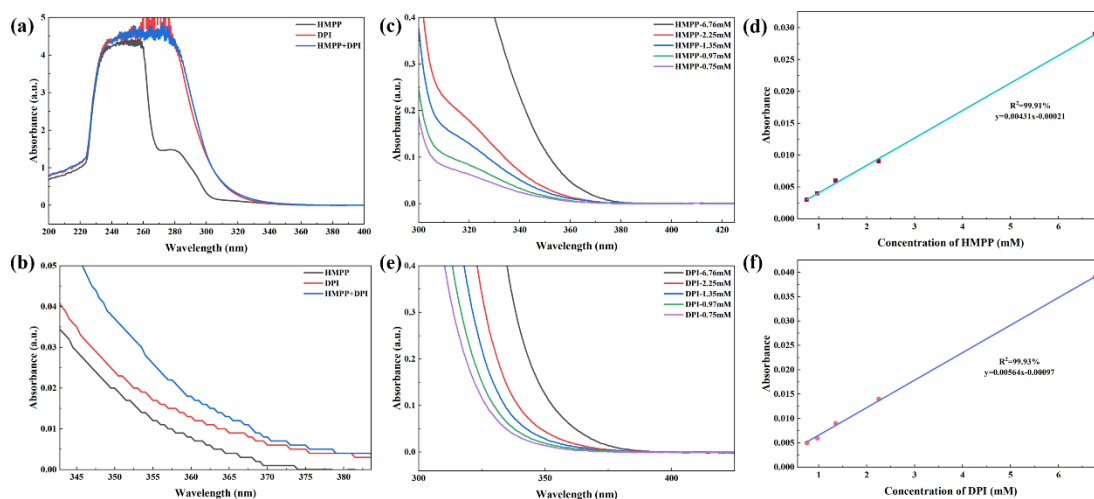


Fig. S2 (a) UV-vis absorption spectra of HMPP, DPI, and their mixture; (b) enlarged view of the absorption spectra at 365 nm; (c) absorption spectra of HMPP at various concentrations; (d) calibration curve for HMPP concentration versus absorbance; (e) absorption spectra of DPI at various concentrations; (f) calibration curve for DPI concentration versus absorbance.

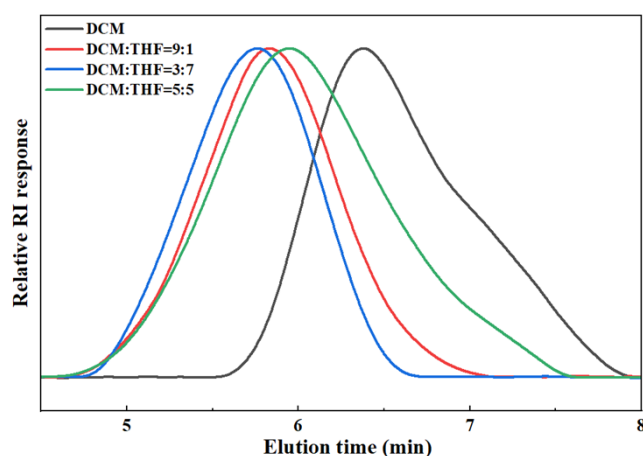


Fig. S3 GPC curves of P(PEG-AME) via FRPCP at different THF concentrations.

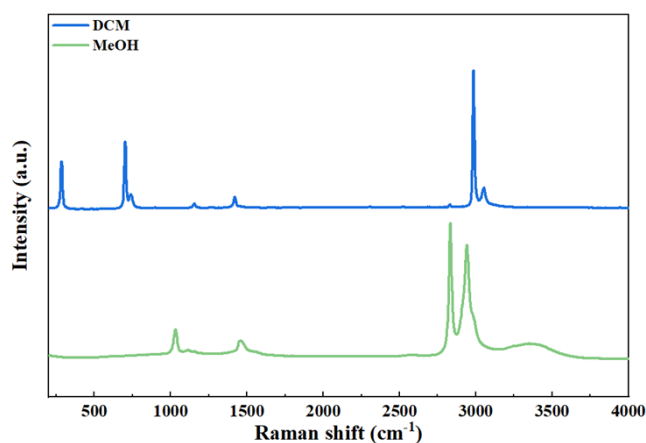


Fig. S4 Raman spectra of DCM and methanol.

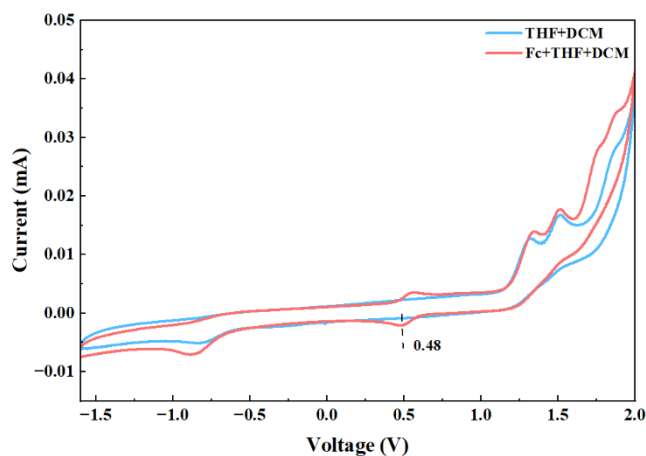


Fig. S5 Cyclic voltammogram of Fc in DCM:THF = 7:3.

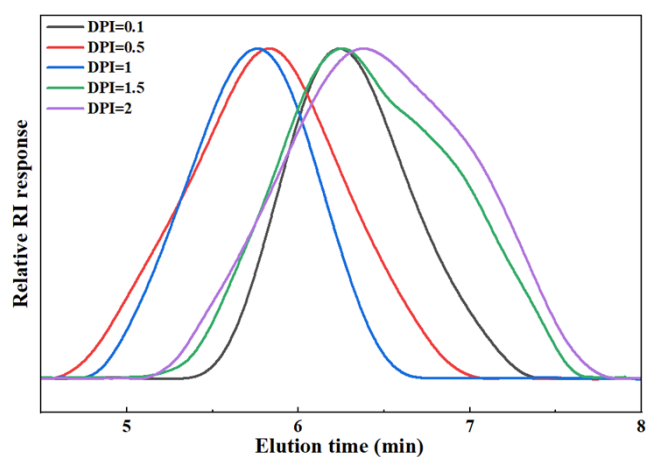


Fig. S6 GPC curves of P(PEG-AME) via FRPCP at different DPI concentrations.

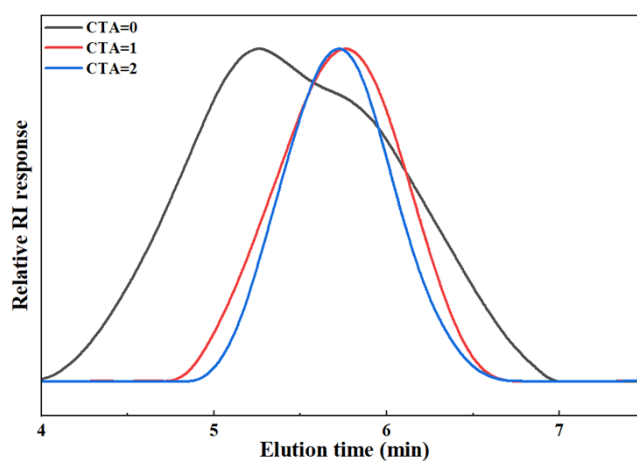
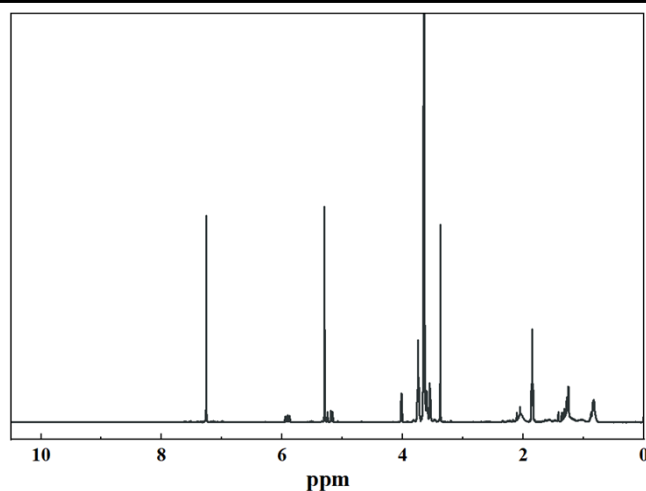


Fig. S7 GPC curves of P(PEG-AME) via FRPCP at different DL-Met concentrations.

Table S2 Condensed Fukui function calculation results for DL-methionine

Atom	q(N)	q(N+1)	q(N-1)	f^-	f^+	f^0	CDD
1(C)	-0.0861	-0.1338	-0.0413	0.0449	0.0477	0.0463	0.0028
2(H)	0.0451	-0.0163	0.0814	0.0364	0.0614	0.0489	0.0250
3(H)	0.0346	-0.0242	0.0790	0.0443	0.0588	0.0516	0.0145
4(H)	0.0352	-0.0235	0.0792	0.0440	0.0587	0.0514	0.0147
5(C)	-0.0523	-0.0580	-0.0232	0.0291	0.0058	0.0174	-0.0233
6(H)	0.0328	0.0132	0.0674	0.0346	0.0196	0.0271	-0.0150
7(H)	0.0347	0.0241	0.0619	0.0271	0.0106	0.0189	-0.0165
8(C)	0.0194	-0.0045	0.0386	0.0192	0.0239	0.0215	0.0048
9(S)	-0.0447	-0.1331	0.3460	0.3907	0.0884	0.2396	-0.3023
10(C)	-0.0510	-0.0713	-0.0340	0.0170	0.0203	0.0186	0.0033
11(H)	0.0335	-0.0119	0.0467	0.0131	0.0454	0.0293	0.0323
12(H)	0.0326	0.0153	0.0504	0.0178	0.0173	0.0175	-0.0006
13(H)	0.0373	0.0047	0.0567	0.0194	0.0327	0.0260	0.0133
14(C)	0.2024	0.0621	0.2127	0.0103	0.1403	0.0753	0.1300
15(O)	-0.2850	-0.4246	-0.2424	0.0426	0.1396	0.0911	0.0970
16(O)	-0.1651	-0.2386	-0.1471	0.0180	0.0734	0.0457	0.0554
17(N)	-0.2001	-0.2368	-0.1059	0.0941	0.0368	0.0654	-0.0574
18(H)	0.1795	0.1311	0.2015	0.0221	0.0483	0.0352	0.0263
19(H)	0.0987	0.0539	0.1418	0.0431	0.0447	0.0439	0.0016
20(H)	0.0984	0.0721	0.1306	0.0321	0.0263	0.0292	-0.0059

**Fig. S8** ^1H NMR spectrum of the non-quenched P(PEG-AME) product obtained via FRPCP.

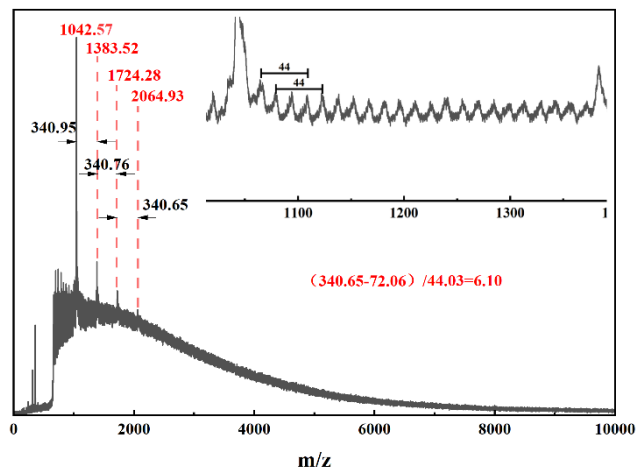


Fig. S9 Original MALDI-TOF MS of PEG-AME-FRPCP.

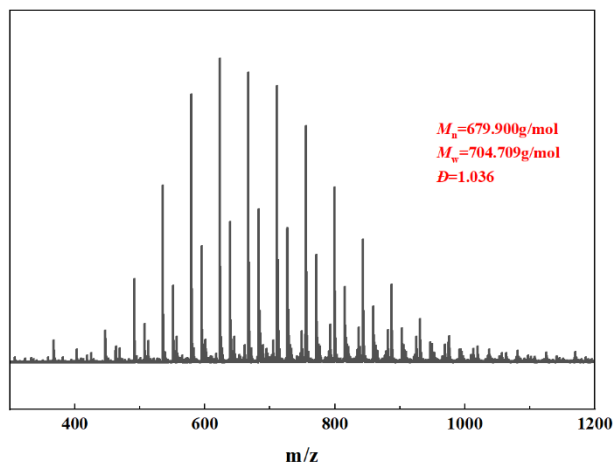


Fig. S10 MALDI-TOF MS of PEG-AME.

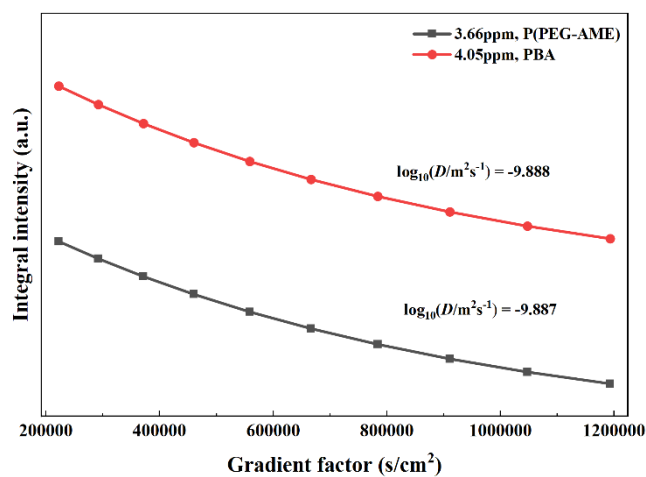


Fig. S11 Integral attenuation fitting of selected DOSY resonances for PBA-*b*-P(PEG-AME).

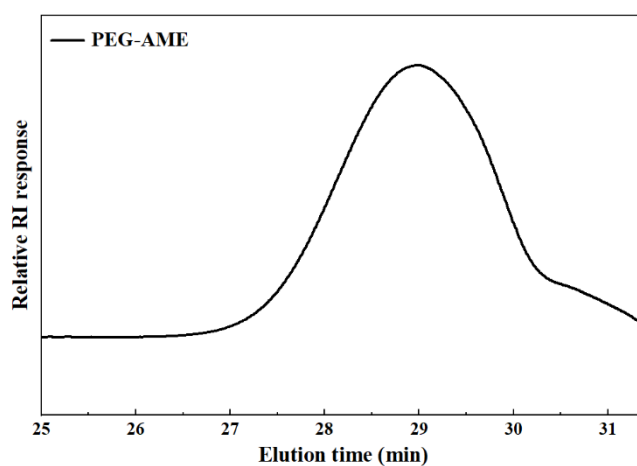


Fig. S12 GPC curve of the crude block copolymer product without purification.